Non-destructive Testing and Process Control Using X-ray Methods and Radioisotopes

M. Kröning, Th. Jentsch[1], M. Maisl, H. Reiter

Fraunhofer Institut für Zerstörungsfreie Prüfverfahren IZFP,

Gebäude 37, D-66123 Saarbrücken

[1] Fraunhofer Institut für Zerstörungsfreie Prüfverfahren IZFP,

Einrichtung für Akustische Diagnose und Qualitätssicherung,

Krügerstraße 22, D-01326 Dresden

Abstract

This paper discusses the potential of two and three-dimensional computed X-ray tomography (CT), computed laminography (CL), and radiotracer techniques. The first and second methods non-destructively make images of the density distribution of cross-sections or of the total volume, while the third method is used in industry to investigate mass transport and mass distribution. The principles of the methods are given and examples for their application are discussed.

X-ray Techniques

2D-Tomography

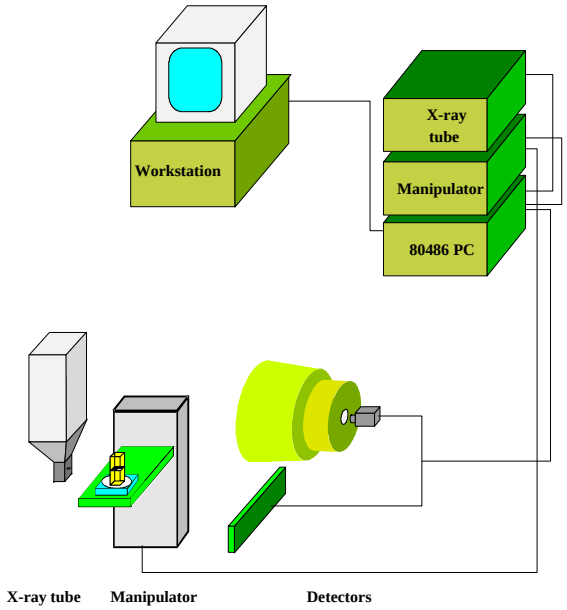

Figure 1: Sketch of the x-ray inspection system

Radiography is a projection technique that gives a shadow projection of the object. All details of the three-dimensional object are superimposed onto the detector. Due to this projection technique, information about the depth of an imaged structure is not possible to discern from a single radiogram. Twenty-two years after the discovery of x-rays, Radon mathematically showed that it is possible to calculate the density distribution of an object from its x-ray projection [1]. Based on this principle, 2D-tomography was developed for medical applications [2]; 2D-tomography reconstructs the attenuation values of single planes inside the object. In the last decade, industrial systems have been developed and applied for the investigation of industrial components. IZFP's system is based on a modular x-ray inspection system. The modular x-ray inspection system has been developed using a microfocus x-ray tube as the radiation source and a line detector or an image intensifier with a CCD camera and image processor as the detection system to inspect low absorbing parts. The flexibility of the system allows the application of different x-ray methods: digital radiography, two and three-dimensional computed tomography (µCT and 3D-CT), and computed laminography (CL). Figure 1 shows a sketch of the system.

The micro-focal x-ray tube was chosen because of the possibility to use the direct magnification technique. The x-ray tube is operated at up to 200 kV and 3 mA (maximum 320 W). The line detector that is applied for digital radiography, µCT, and CL, consists of 1024 photo diodes covered by a 400 µm thick Gadox scintillator.

The image intensifier is used not only for digital radiography and 3D-CT, but also for CL and µCT. For the different reconstruction techniques, projection data are transferred to a PC or a workstation.

The reconstruction of a two-dimensional image requires only one-dimensional projection data. For that reason, the cone beam is reduced to a fan beam by collimators resulting in a reduction of scattered radiation. Using the line detector, the pixel size “w” is determined by the object diameter “D” to w = D. Due to the small spot size of 10 µm and the accuracy of the manipulation system, the smallest pixel size realized is about 10 µm. The maximum diameter of the reconstructed cross sections amounts to 350 mm due to the length of the line detector (460 mm) [3].

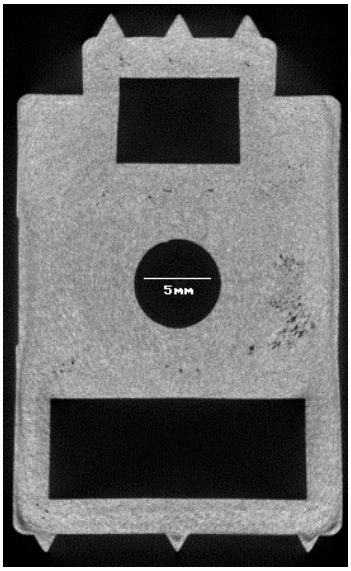

Figure 2: Fiber-reinforced plastic, pores

Figure 2 displays the reconstructed cross-section of a fiber-reinforced plastic part with porosity and inhomogeneous density distribution, especially near the surface.

Figure 3 shows the tomogram of a plate of carbon fiber-reinforced plastic after impact damage. The plate consists of six layers of woven carbon roving. Due to the impact, the layers are broken, which is clearly visible in Figure 3. The second layer is destroyed by the impact.

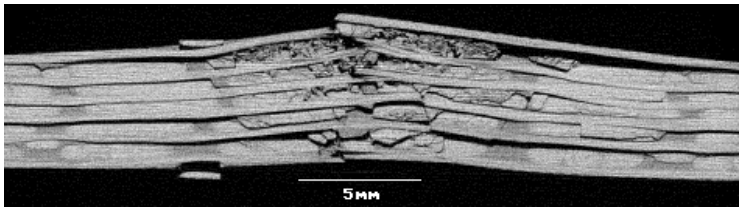

Figure 3: Carbon fiber-reinforced plastic with impact damage

3D-Tomography (3D-CT)

In 3D x-ray-computed tomography (3D-CT), not only one plane but also the volume of an object is reconstructed using the 2-dimensional (2D) radiographic projections of the object. For 3D-CT, typically cone beam geometry is used. The object is rotated in a x-ray cone beam produced by a x-ray tube. Many 2D projections under different angles are measured by a 2D-detector system, e.g. an image intensifier and a CCD camera, and are digitized by an image frame grabber system. From all 2D projections, the density distribution or, more correctly, the distribution of the linear attenuation coefficients inside the object is reconstructed using mathematical reconstruction algorithms. In the past, different reconstruction algorithms for the cone beam geometry have been developed [4,5].

Figure 4: Battery, 3D-CT, outside view

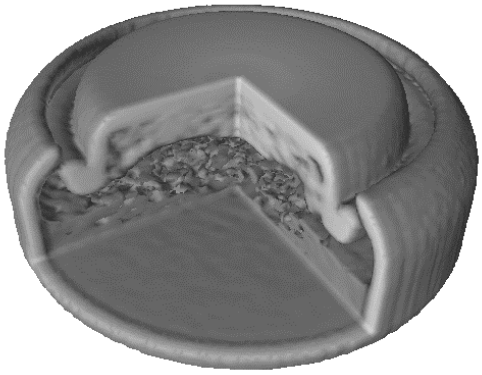

Figure 5: Battery, 3D-CT, inside view

Figures 4 and 5 show two three-dimensional views of the reconstruction of a small battery. Figure 4 visualizes only the outer contour of the battery. In Figure 5, the battery is cut open by software, showing the porous structure of the electrodes.

Computed Laminography (CL)

In the case of computed tomography, the objects have to be irradiated from all directions. This is not always possible, for example, in the case of flat components or limited access to the component to be investigated, but laminography can overcome these difficulties. Classical laminography is based on the relative motion of the x-ray source, the detector, and the object. The x-ray source and the detector are moved synchronously in opposite directions. Due to that correlated motion, the location of the projected images of points within the object also move. However, points from a particular plane will be projected always at the same location onto the detector and therefore imaged sharply. The major handicap of classical laminography is the complicated system setup. In each measurement, only one plane, the focal plane, is imaged sharply; other planes must be inspected consecutively by displacing the object vertically.

We have developed a new laminography method, the computed laminography, which only requires a simple linear translation of the object through the fan beam of a x-ray source. Both x-ray source and detector remain stationary as shown in Figure 6 [6].

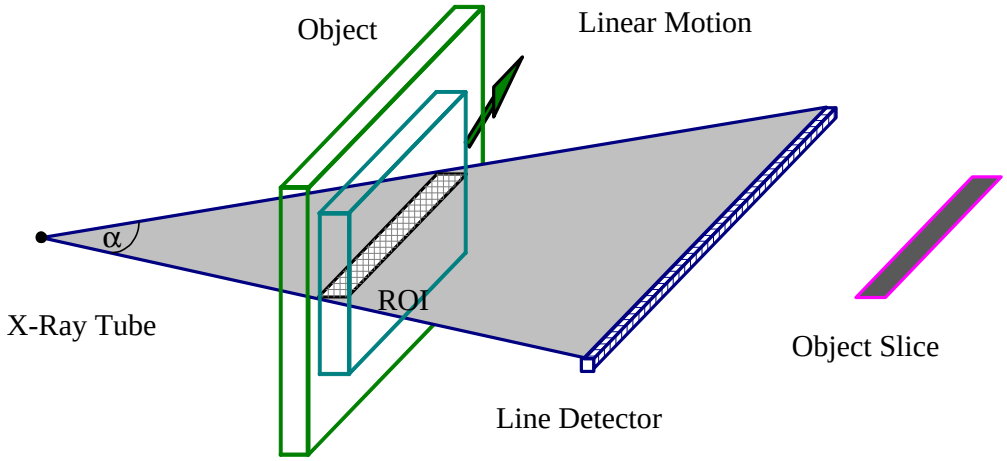

Figure 6: Principle of computed laminography

The object is irradiated by the x-rays under different angles from the fan beam with an opening angle α. As the object is moved through the x-ray fan beam, the elements of the detector get successive information of a given volume element of the object under consecutively changing angles. Using a flat two-dimensional detector and the cone beam of the x-ray tube, the digital stored projections will then contain structure information of all object planes. The situation of CL is equivalent to a computed tomography (CT) with a limited aperture. This allows us to reconstruct cross-sections of the object using CT algorithms like ART [7], which removes the washout effect of classical laminography. In addition, the use of algebraic reconstruction techniques allows for easy addition of a priori information, which reduces the reconstruction time and the artifacts caused by the limited access.

Figure 7 shows an example of the higher quality images obtained with CL in comparison to classical laminography, where a surface mounted device was examined with classical laminography (images a. and c.) and computed laminography (images b. and d.). The computed laminography images were obtained by taking a slice through many individual reconstructions perpendicular to the surface of the board. The classical laminography images only the lead frame (Fig. 7a); the connecting wires cannot be resolved. The CL image (Fig. 7b) of the same region is in general much sharper and shows clearly the connecting wires. Figures 7c and 7d show a cross section in the plane of the circuit board. In Figure 7c, only the solder joints are clearly visible but not with their correct geometry. CL (Figure 7d) shows this much clearer with further details such as tracks, feed-through and two pores within the solder joints are resolved.

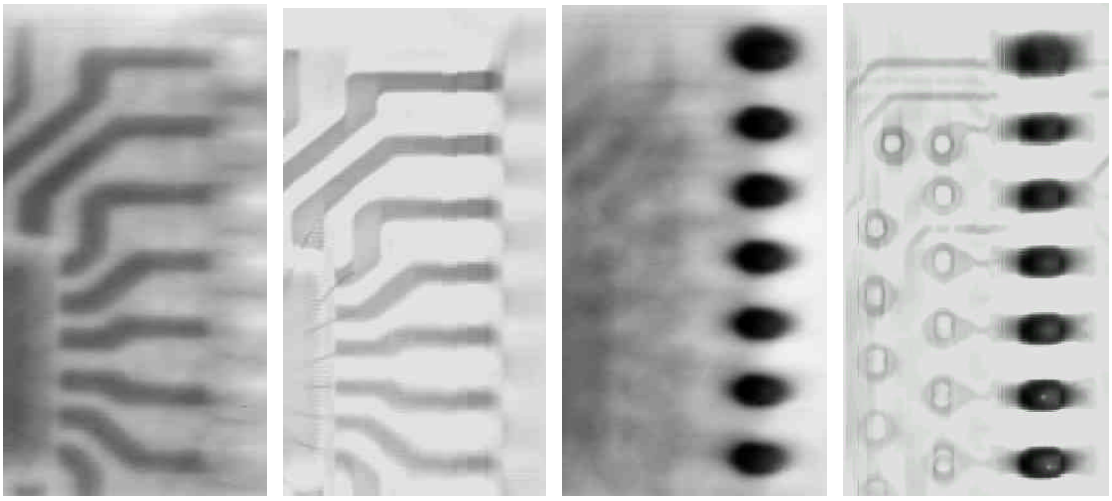

a) b) c) d)

Figure 7: Laminography of a surface mounted device

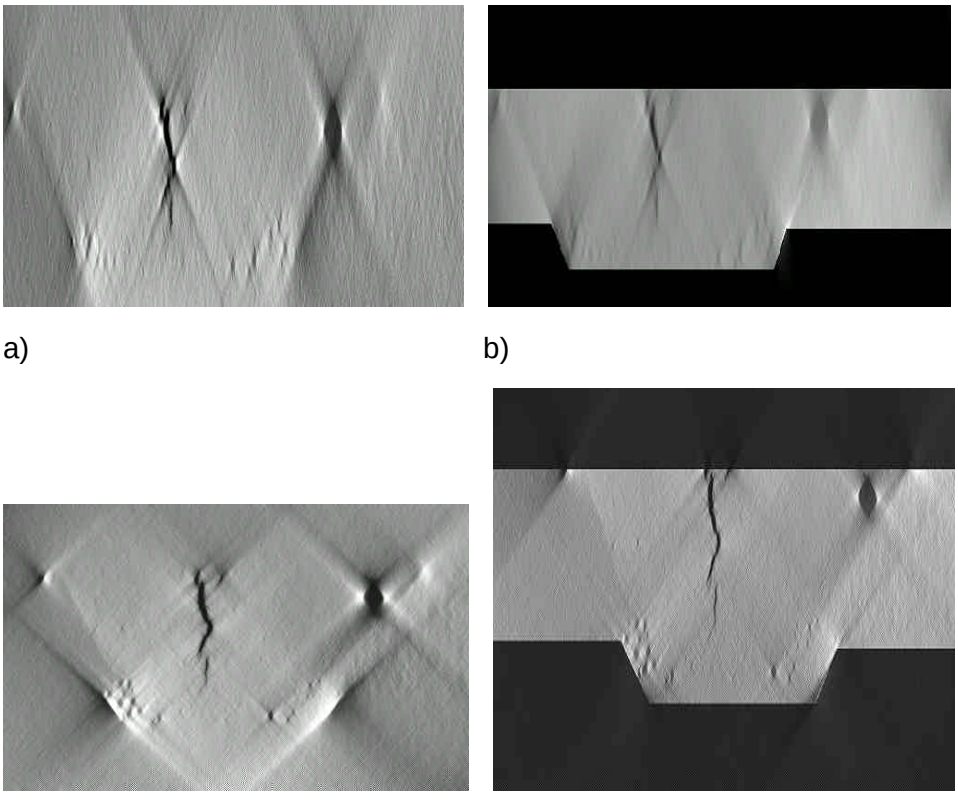

a) b)

c) d)

Figure 8: Aluminum seam weld with cracking and porosity

Computed laminography yields images of an examined object layer by layer with a higher sensitivity to crack-like flaws as compared to radiography. This is caused by the reconstruction of the image from different projections measured under different angles. Moreover, this reduces the noise of the image because of the averaging effect.

In Figure 8, a CL-image of an aluminum seam weld with cracking and porosity is shown. In Figure 8a, the aperture angle of the fan beam is approximately 30°; in Figure 8c, it is 90°. It is evident and clearly visible that a bigger aperture angle leads to better results in the reconstruction. Figures 8b and 8d show reconstruction using the object surroundings as a priori information. The artifacts are minimized and the position of the crack and the pores inside the weld can easily be detected.

Radiotracer Techniques

Traditionally, radiotracer techniques come from medical and industrial research and are used for the investigation of mass transport and mass distribution. In the present paper, examples from our institute describe the radiotracer's use in investigating mass transport in matrices and industrial plants.

Investigations of mass transport in matrices

In order to study penetration of specific substances into solid matrices or in containers with non-transparent walls, radiotracer methods are exclusively applied. To demonstrate this unique possibility, two examples are described herein, i.e. the investigation of transport of liquids and of transport of salt into building materials, and the investigation of transport of a NaCl solution into a bentonite bed.

Transport of liquids and of salts into cracked and intact building materials

Buildings, in particular the outer walls and the foundation, are affected by water and solved ions stimulating corrosion. Within various investigations at our institute, the penetration behavior of substances damaging buildings into intact as well as into cracked building materials was studied. Mainly samples of concrete and mortar of various compositions were studied.

Depending on the goal intended by the investigation, various radiotracers were used. Chloride is the compound representing the corrosion-stimulating ions by which buildings are damaged. As far as chlorine is concerned, besides the long-life isotope ^{36}Cl (with a half-life of 300,000 years) which is only a beta emitter and cannot be used for non-destructive investigations, only comparatively short-lived gamma radiators of a half-life of some minutes exist, and the investigations on the transport of salt were predominantly made using the ^{72}Br isotope.

Investigating water transport, isotopes of oxygen or of hydrogen cannot be taken, as they are either too short-lived (half-life of ^{15}O, for example, is 2 minutes) or they are pure beta emitters. Using ^{99m}Tc, which is present in aqueous solution in form of pertechnetate as anion, good results were achieved.

The penetration behavior into intact building materials was investigated using cubes of a side length of 150 mm or drill cores of a diameter of 150 mm. To investigate the transport behavior in the crack of a building component, prisms of (100 x 100 x 300) mm^3 were used, in which real cracks of some tenths of a millimeter were generated. Using two slit-shaped collimated scintillation counters arranged laterally at the crack, penetration of the traced liquid filled by means of a reservoir was observed in two depths of cracks. In addition, information on the ion exchange and the kinetics of saturation of the lateral surfaces of the crack was provided when the activity concentration at the end of the crack was determined.

Liquid and salt penetration into intact building materials was observed using slit shaped collimated scintillation counters, too. Applying samples of portable dimensions allowed using modern detection systems of nuclear medicine like the gamma camera or Single Particle Emissions Computerized Tomography (SPECT). Figure 9 shows the SPECT record of a drill core. For a period of 24 hours, over this core's base area pertechnetate traced water influenced by gravity was poured and remained. In this figure, the distance between the intersecting planes is 4mm, so in this case a penetration depth of about 20mm was determined.

Determination of the maximum penetration depth of NaCl solution into a bentonite bed in a cylindrical pressure tank

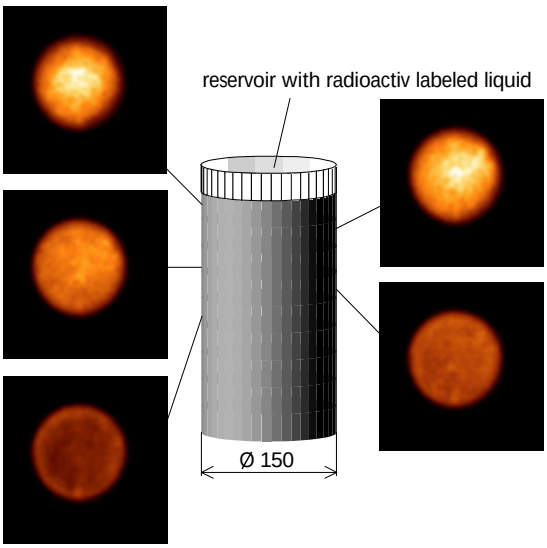

Figure 9: SPECT record of a drill core, poured with aqueous $Na^{99m}TcO4$ solution

For the final disposal of hazardous waste, underground waste disposal sites are increasingly being used. Shafts and tunnels no longer used in mining are filled with leak-proof compacted hazardous waste and are then sealed up. These seals are subject to considerable mechanical stress and, therefore, must be of high strength. To seal final disposals of hazardous waste, it is recommended to use bentonite - a natural mineral that is highly capable of swelling. The mineral mixture is filled in dry state and it swells when water is poured over it, so a tight seal is formed. This seal can be considerably mechanically stressed, because bulking in the shaft or tunnel is prevented from taking place.

As it is expected that in the final disposals liquids penetrate, usually as a saturated NaCl solution, NaCl solution is used to form the seal in order to achieve the swelling of bentonite. Measuring the temporal course of the maximum penetration depth of NaCl solution as a function of the pressure regime allows examination of the theoretically determined penetration behavior and, thus, to draw conclusions with regard to the achieved mechanical strength.

As tracer nuclide ^{22}Na can be taken, because of the emitting of high-energy gamma radiation and positrons and a half-life time of 2.6 years.

The front of the solution was observed using two slit shaped collimated NaI (TI) scintillation counters that were reproducibly moved up and down using a positioning system along the cylindrical steel cylinder where the tests were performed. As the aim of our investigations was to determine the temporal course of the maximum penetration depth of the solution, both detectors were tilted so that the upper border of the area of detection defined by the collimating slit forms a horizontal surface, i.e. it is rectangular to the axis of the cylinder. Therefore, it was easy to determine the depth where there is no penetration of the solution. To determine the concentration of the solution in the "layers" above, two neighboring measured values are subtracted.

In addition, when spectra-metrically registering the measured signals a qualitative statement can be made on the temporal course of the distribution of the solution within a cylinder cross-section: radiation arising at positrons annihilation is of less energy than gamma radiation of the Na isotope (511, 1275 keV, respectively). Consequently, annihilation radiation is attenuated to a greater extent (the bentonite bed causes this, too) than the high-energy gamma radiation. When the measured signals always come out of the same depth of the cylinder, the ratio of the portion of the two radiation sources at the measured signal must remain unchanged.

However, it was found out that these ratios change: at first, the energy-enriched signal prevails and, progressively, the portion of the signal low in energy increases. It can be concluded that the transport process at first takes place predominantly in the central part of the cross-section and later, the marginal zones participate in the transport process. Thus, it was proven that a negative effect at the marginal zone that was expected occasionally, e.g., the preferred penetration at the marginal zone of the bed by flowing down at the interior steel wall - did not occur in this case.

Investigations of mass transport in industrial plants

Mass transport investigations of continuous processes in industrial plants are an important field of application for radioactive indicators. In these investigations, materials are often measured concerning residence time and distributions of residence time in definite apparatuses.

Residence time distribution

Measurements in the field of household waste pyrolysis with regard to residence time distributions in various parts of a rotating low-temperature carbonization drum.

Pyrolysis reliably carried out in a rotating cylinder is the basis for the functioning of the low-temperature carbonization plant. Extensive knowledge on the processes in the low-temperature carbonization drum is the basis to draw up real models and to appropriately master this process stage.

In process modeling, three processes should be taken into consideration: processes of heat transfer, of chemical reaction, and of mass transport. The models must be tested by process analyses and modified if necessary. In this case, testing of processes of mass transport - if

possible in different parts of the rotary drum - are of special importance, because the transport properties of the solid material passing the rotary drum show considerable change, caused by the chemical reaction.

The necessary information was acquired by residence time measurements using radiotracers in an experimental plant. As far as the complexity of the mass system of household waste is concerned, a model substance was chosen to carry out the mass transport investigations that is transported in the front part of the pyrolysis rotary drum like household waste, but otherwise shows transport properties of the pyrolysis coke. As a result of extensive preliminary investigations, expanded shale fragments were chosen. This material is sufficiently temperature-resistant and abrasion-resistant; in addition, it is of a porous structure, so the radiotracer absorbs preponderantly at internal surfaces. Taking into account that the solid material temperatures reach up to 550 °C, ^{113m}In was selected to be used as a tracer nuclide. In the tests, the influence of the drum RPM and of the waste mass flow on time required for the transport was investigated and, in addition, the influence of various particle sizes.

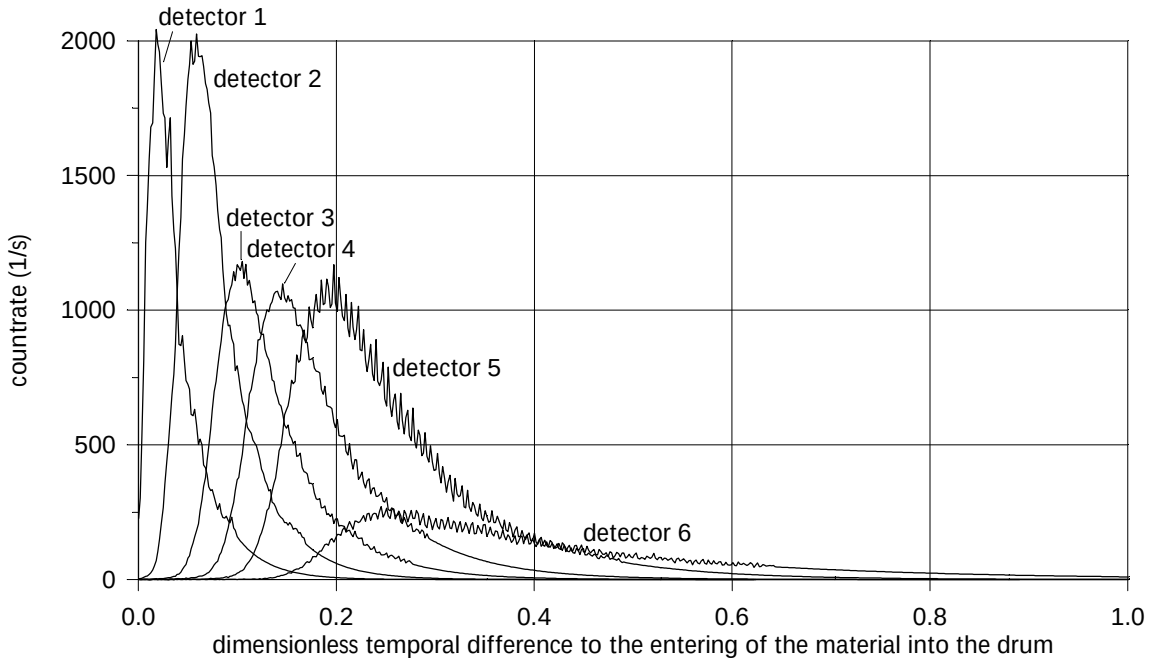

Figure 10: Residence time distributions, measured at six positions of the rotary drum of an experimental low-temperature carbonization plant

In Figure 10, residence time distributions (after background and half-life correction) measured at six positions of the rotary drum are shown. The modal and median values as well as the standard deviation were determined. On this basis, for each part of the rotary drum, the

probable and average values of residence time, the solid materials transporting rates, the equivalent numbers of compartments, the Bodenstein numbers, and the degree of filling were detected in the investigated parts of the rotary drum. In addition, the dependencies of these parameters on the drum RPM, the solid mass flow and the particle size were determined.

Measurement of residence time distributions in various segments of the rotating cylinder in paint pigment production

In technology, pearl pigments based on mica are widespread. They are applied in making plastics, printing inks, cosmetics and car finishes. In rotary cylinders, pigments are thermally fixed on the mica particles. The quality of this process is decisive for the paint pigments quality.

To analyze the actual state, residence time distributions were measured in different parts of two rotating cylinders of the same type. In one rotary kiln, two tests were performed using one paint pigment. In the other kiln, two tests were carried out using a different paint pigment. In all the tests, the operating conditions were alike except for insignificant variations of mass flow.

Tracing was done using ^{113m}In advantageously extracted from the isotope of a radio nuclide generator by precipitating ^{113m}In(OH)3 at the surfaces in a low quantity (10 g) of the paint pigments concerned. The traced pigment quantity was added as a DIRAC-pulse into the mass flow entering the rotary kiln. At 10 positions in each kiln, non-contact scintillation counters measured pulse rate - time - courses in analogy to the wanted residence time distributions in various parts of the rotating cylinder. After the necessary modifications of the measured data, the most probable and average residence time of each distribution was determined. In Figure 11, the average residence time parameters in dependence on the position of measurement are shown.

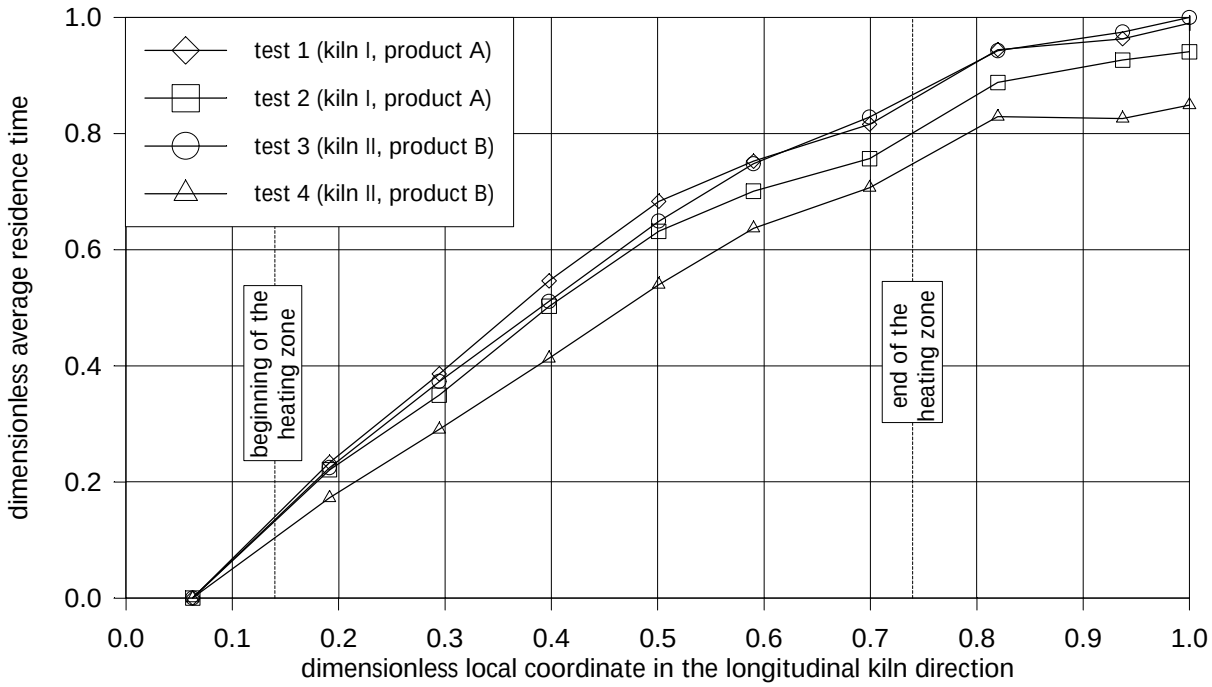

Figure 11: Average parameters of residence time in dependence on the position of measurement at the kiln

There is a good correlation of the measured parameters determined in two tests with one product at one kiln under practically identical conditions. In addition, there is a good agreement of the measuring results and the data acquired at the same kiln using a different product. In the measuring results, divergences are mainly caused by deviations of the operational parameters such as those of the pigment mass flow. In addition, by the measurement, information is provided how the baffles, which form the boundary of the heating zone, influence the mass transport.

Summary

Due to the progress in computer and X-ray detector technology, reconstruction techniques are used more frequently for the nondestructive inspection of industrial components. The computed tomography (2D-CT and 3D-CT) and the computed laminography (CL) image single planes or the volume of the investigated object. These techniques can be seen as nondestructive microscopy, delivering cross-sections. They provide the following:

- detection of small voids that cannot be detected by conventional radiography
- determination of kind, size, geometry, and location of flaws
- display of the density distribution within single planes or the volume
- measurement of distances and dimensioning of details

In contrast to CT, CL needs only access from two sides of the object and is best suited for the inspection of flat components within the electronics industry.

Although there is a rapid development of physical measuring methods in modern industry, traditional radiotracer techniques are applied in areas where other methods and techniques cannot be used. In the future, these traditional techniques will be confronted with tasks that can not be solved advantageously and securely with other measuring methods, and they will succeed again where others have failed as they always have in past decades when these methods have been applied.

References

[1] J. Radon, Ber. Verh. Sächs. Akad. Wiss., Leipzig, Math. Phys. Kl. 69, 262, (1917)

[2] G. N. Hounsfield, Brit. J. Radiol., 46, 1016 - 1022, (1973)

[3] M. Maisl, R. Herzer, in Proc. International Conference on Monitoring and Predictive Maintenance of Plants and Structures, 516-529, (1992)

[4] L. A. Feldkamp, L. C. Davis, J. W. Kress, J. Opt. Soc. Amer., 1, 612,(1984)

[5] J. Buck, PhD thesis, Technical Faculty, University of Saarbrücken, (1996)

[6] J. Zhou, M. Maisl, H. Reiter, W. Arnold, Applied Physics Letters, 68, 3500, (1996)

[7] S. W. Rowland, *in Imaging reconstruction from projections*, (Ed. G. T.